

Supporting Information

NIR excited superoxide procreators to eradicate the tumor cells by Targeting Lyso-membrane

Bhaskar Gurram,^a Miao Li,^a Mingle Li,^a Kalayou H Gebremedhin,^a Wen Sun,^a Jiangli Fan,^a Jingyun Wang,^b and Xiaojun Peng^{a*}

^aState Key Laboratory of Fine Chemicals and ^bSchool of Life Science and Biotechnology,
Dalian University of Technology, 2 Linggong Road, Hi-tech Zone, Dalian 116024, P.R. China.

Corresponding Author Email: * pengxj@dlut.edu.cn Tel/Fax: +86-411-84986306

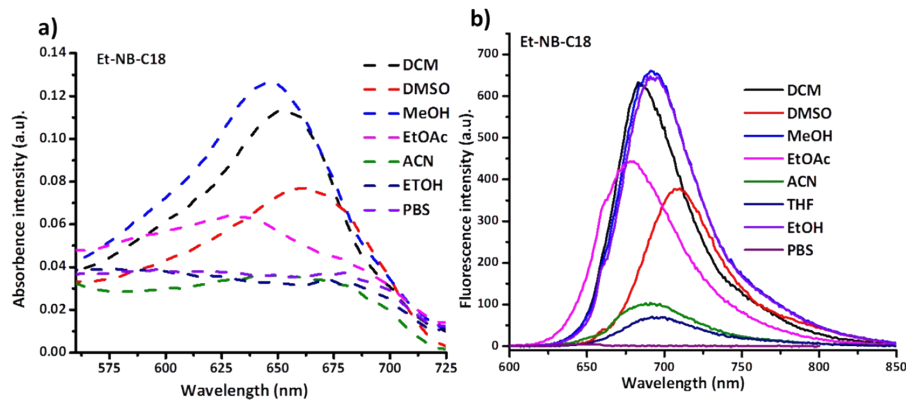


Figure S1. The absorbance (a) and emission (b) spectra of Et-NB-C18 (4 μM) in different solvents.

Solvent	$\lambda^{\text{abs}}(\text{nm})^{[a]}$	$\lambda^{\text{em}}(\text{nm})^{[b]}$	$\Delta\lambda(\text{nm})$	$\epsilon \times 10^5 \text{L/(M}^{-1}\text{cm)}^{[c]}$	$\Phi^{[d]}$
DCM	662	700	38	0.447	0.442
DMSO	662	720	58	0.337	0.203
MeOH	654	702	48	0.586	0.168
EtOAc	640	675	35	0.261	0.363
THF	662	710	48	0.174	0.148
ACN	662	700	38	0.176	0.189
EtOH	660	695	35	0.488	0.167
PBS	671	700	29	0.089	0.026

[a, b] The absorption and emission wavelength; [c] Fluorescence quantum yield; [d] Molar extinction coefficient.

Table S1. Photophysical properties of Et-NB-C18 in various solvents

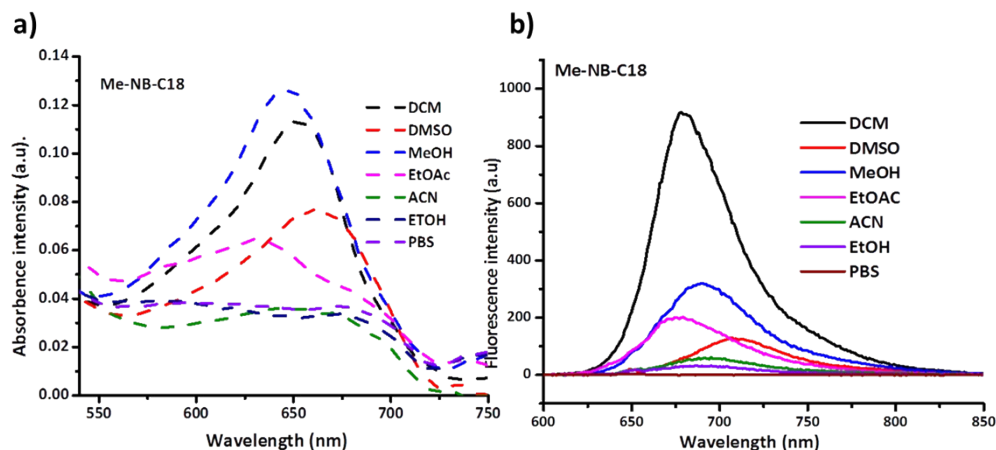


Figure S2. The absorbance (a) and emission (b) spectra of Me-NB-C18 (4 μM) in different solvents

Solvent	$\lambda_{\text{abs}}(\text{nm})^{[a]}$	$\lambda_{\text{em}}(\text{nm})^{[b]}$	$\Delta\lambda(\text{nm})$	$\epsilon(\times 10^5 \text{L}/(\text{M}^{-1}\cdot\text{cm}))^{[c]}$	$\Phi^{[d]}$
DCM	651	694	43	0.282	0.453
DMSO	662	710	48	0.323	0.160
MeOH	649	690	41	0.312	0.151
EtOAc	637	675	38	0.157	0.274
ACN	645	690	45	0.091	0.197
EtOH	637	696	59	0.084	0.167
PBS	636	700	64	0.176	0.015

[a, b] The absorption and emission wavelength; [c] Fluorescence quantum yield; [d] Molar extinction coefficient.

Table S2. Photophysical properties of Me-NB-C18 in various solvents

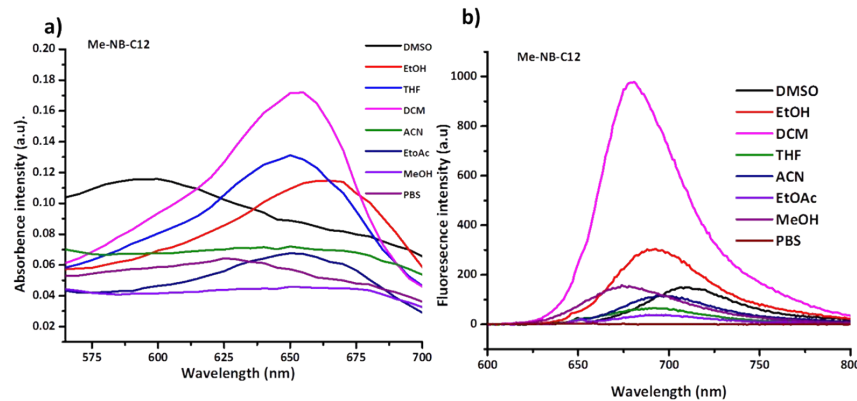


Figure S3. The absorbance (a) and emission (b) spectra of Me-NB-C12 (4 μM) in different solvents

Solvent	$\lambda_{\text{abs}}(\text{nm})^{[a]}$	$\lambda_{\text{em}}(\text{nm})^{[b]}$	$\Delta\lambda(\text{nm})$	$\epsilon(\times 10^5 \text{L}/(\text{M}^{-1}\cdot\text{cm}))^{[c]}$	$\Phi^{[d]}$
DMO	651	710	59	0.287	0.145
EtOH	664	695	31	0.285	0.329
DCM	650	694	44	0.327	0.477
EA	650	700	50	0.114	0.329
THF	654	687	33	0.180	0.095
ACN	650	700	50	0.098	0.211
PBS	651	690	39	0.096	0.017

[a, b] The absorption and emission wavelength; [c] Fluorescence quantum yield; [d] Molar extinction coefficient.

Table S3. Photophysical properties of Et-NB-C12 in various solvents

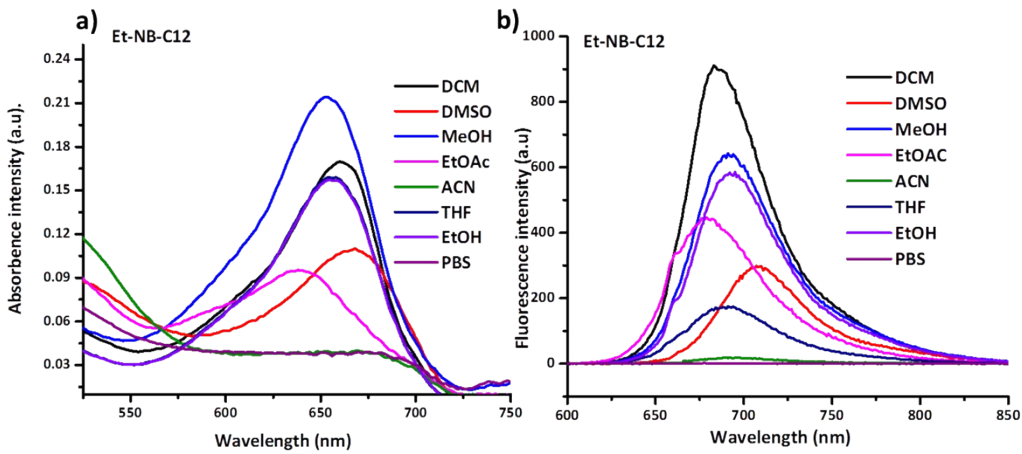


Figure S4. The absorbance (a) and emission (b) spectra of Et-NB-C12 (4 μ M) in different solvents

Solvent	$\lambda_{\text{abs}}(\text{nm})^{[a]}$	$\lambda_{\text{em}}(\text{nm})^{[b]}$	$\Delta\lambda(\text{nm})$	$\epsilon \times 10^5 \text{L}/(\text{M}^{-1} \cdot \text{cm})^{[c]}$	$\Phi^{[d]}$
DMO	662	715	50	0.272	0.202
EtOH	657	700	43	0.392	0.169
DCM	662	696	34	0.422	0.437
EA	655	700	45	0.198	0.364
THF	654	690	36	0.397	0.184
ACN	662	700	38	0.097	0.203
PBS	661	696	35	0.089	0.021

[a, b] The absorption and emission wavelength; [c] Fluorescence quantum yield; [d] Molar extinction coefficient.

Table S4. Photophysical properties of Et-NB-C12 in various solvents

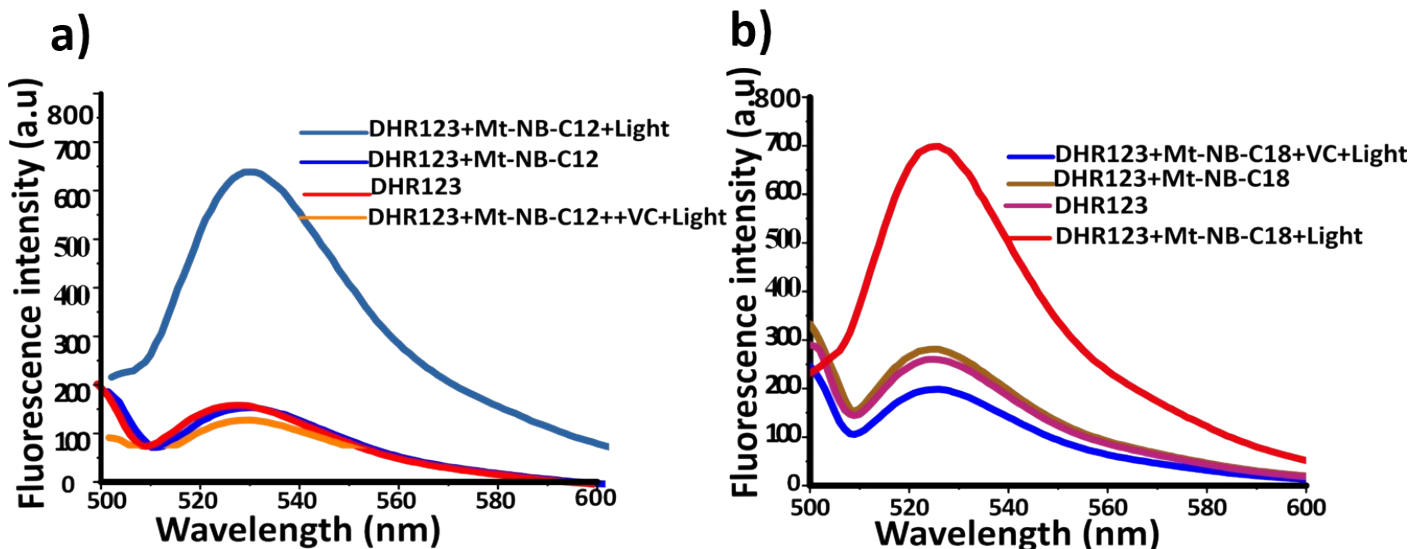


Figure S5. Fluorescence spectra for confirmation of O_2^- using DHR123 with NIR photosensitizers. a-b) Fluorescence spectra for confirmation of O_2^- using DHR123 fluorescence emission spectra at 525 nm after 660 nm irradiation for 8 min with Et-NB-C12 and Et-NB-C18.

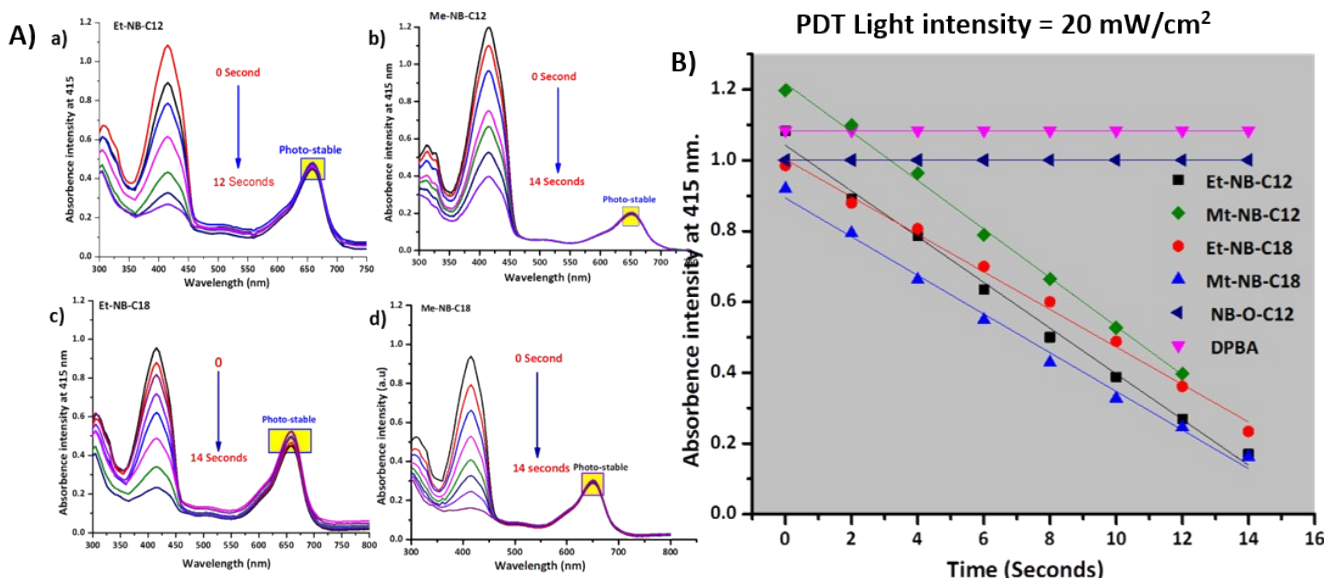


Figure S6. DPBF Photo-degradation decay rate at 415 with NIR photosensitizers. A: a-d) Assessment of DPBF Photo-degradation decay rate at 415 with NIR photosensitizers under illumination of λ_{ex} 660 nm of irradiation; B) DPBF absorbance decay rates at 415 nm as a function of irradiation time under light illumination at 660 nm (20 mW/cm²) in the presence of NIR photosensitizers.

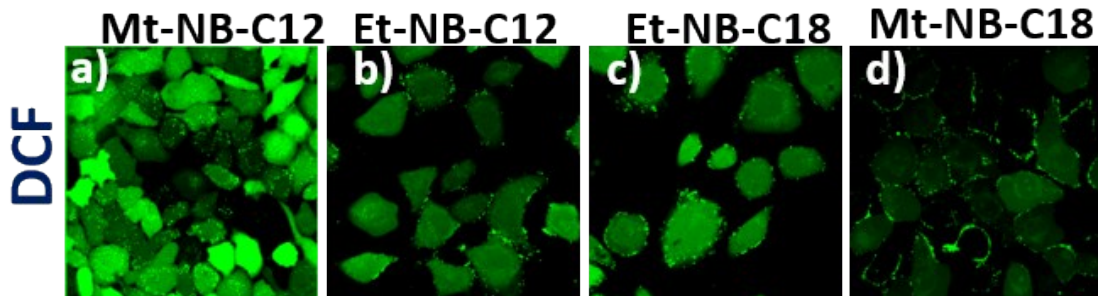


Figure S7. DCF assay. a-d) Cells were stained with DCF before irradiation at 660 nm of light (24 mW/cm²) with NIR photosensitizers. Scanning range of DCF at λ_{ex} 488 - λ_{em} 500-550 nm.

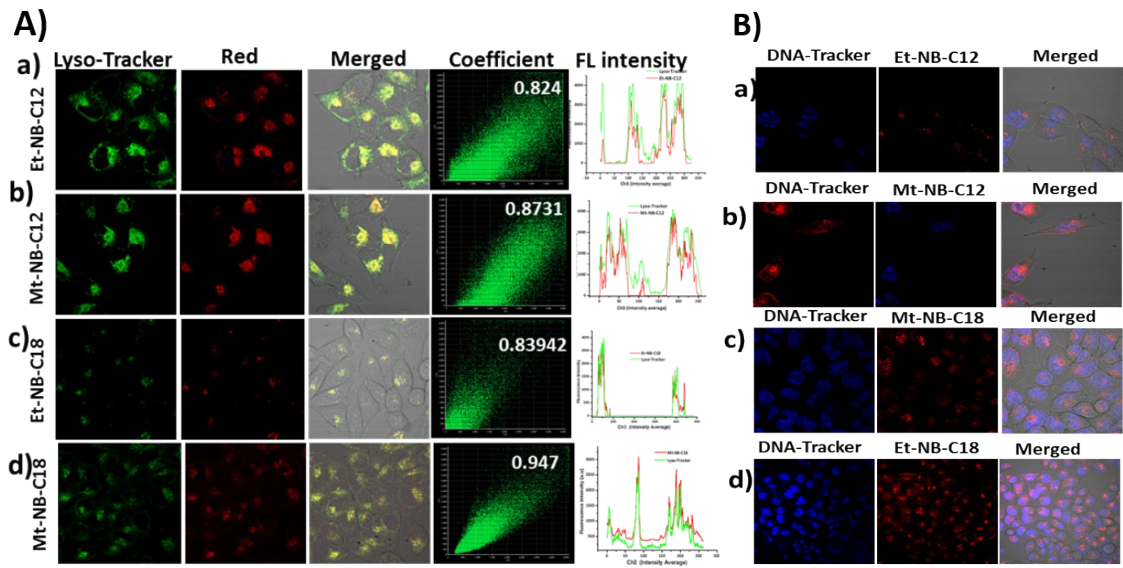


Figure S8. Co-localization of NIR photosensitizers with lyso- tracker green and Hoechst 33342 blue. A: a-d) Co-localization of lyso- tracker green ($\lambda_{\text{ex}} 488 - \lambda_{\text{em}} 510\text{-}540$ nm) with NIR cationic photosensitizers ($\lambda_{\text{ex}} 635 - \lambda_{\text{em}} 670\text{-}720$ nm); B: a-d) Co localization of Hoechst 33342 blue ($\lambda_{\text{ex}} 488 - \lambda_{\text{em}} 515\text{-}540$ nm) with NIR photosensitizers ($\lambda_{\text{ex}} 660 - \lambda_{\text{em}} 670\text{-}720$ nm).

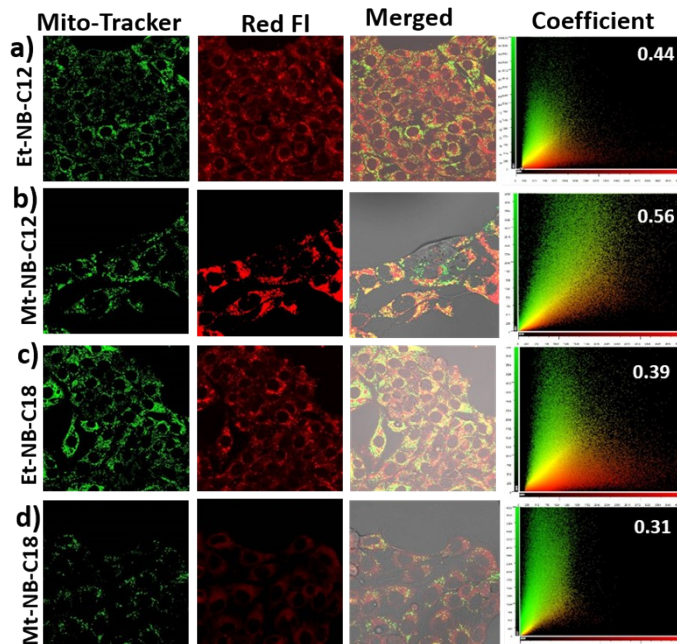


Figure S9. Co-localization of NIR photosensitizers with mito- tracker green. a-d) Co-localization of mito- tracker green ($\lambda_{\text{ex}} 488 - \lambda_{\text{em}} 500\text{-}540$ nm) with NIR cationic photosensitizers ($\lambda_{\text{ex}} 635 - \lambda_{\text{em}} 670\text{-}720$ nm);

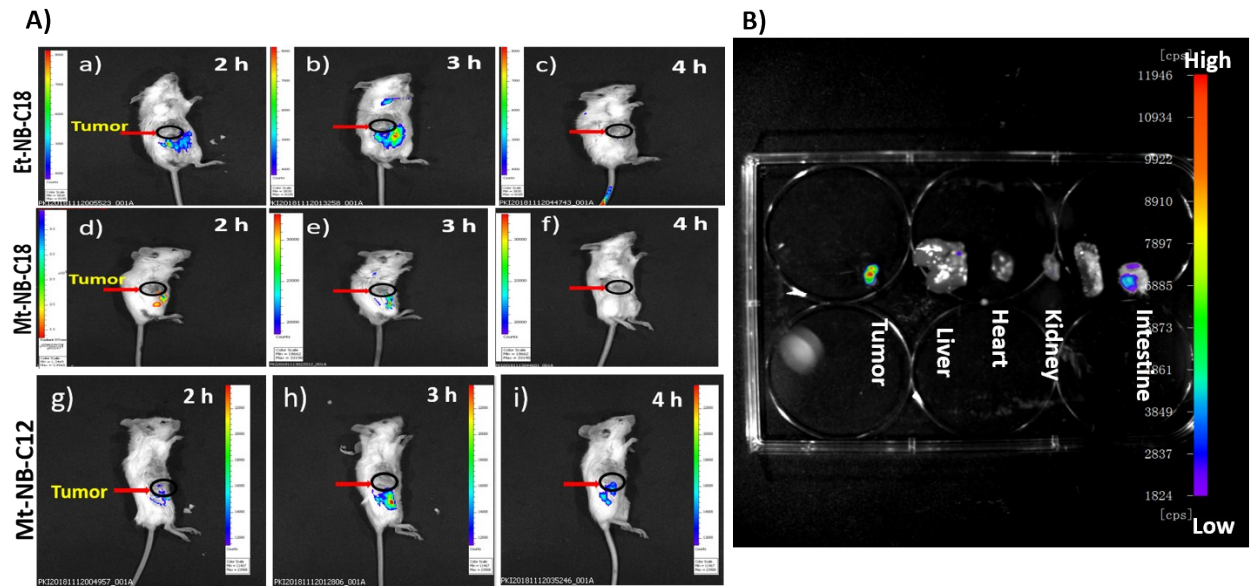


Figure S10. *In vivo* imaging of tumor tissue and vital mice organs. *In vivo* imaging of tumor tissue (A) and (B) vital mice organs (liver, heart, kidney, spleen and intestine) at 4 h of intratumoral injection of NIR photosensitizers (λ_{ex} 660 - λ_{em} 670-720 nm).

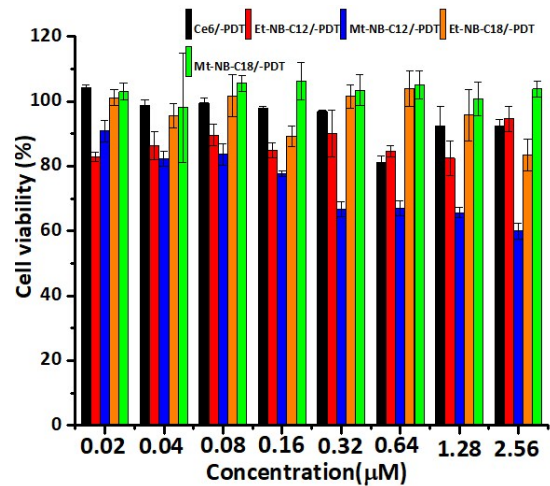


Figure S11. Dark toxicity of NIR photosensitizers (after 12 h of incubation)

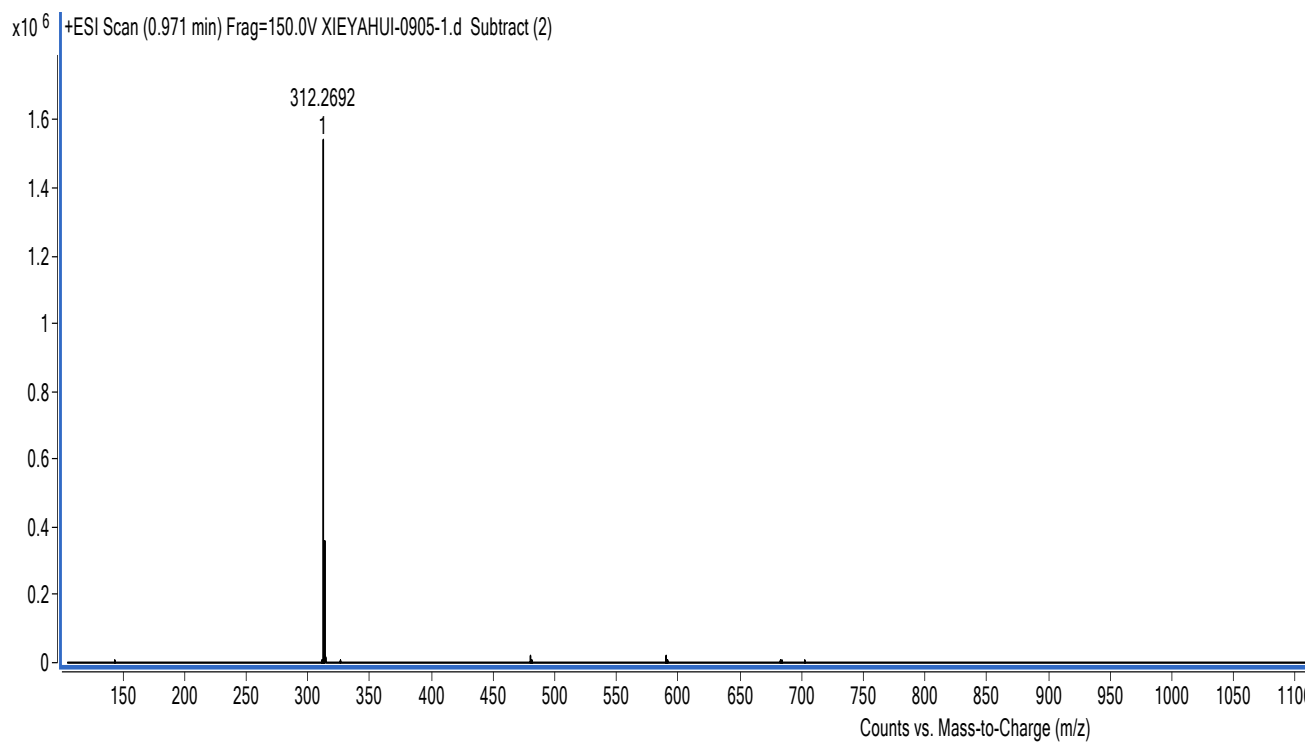


Figure S12. Mass of **1** $\mathbf{R}_1 = \mathbf{NB-C12}$

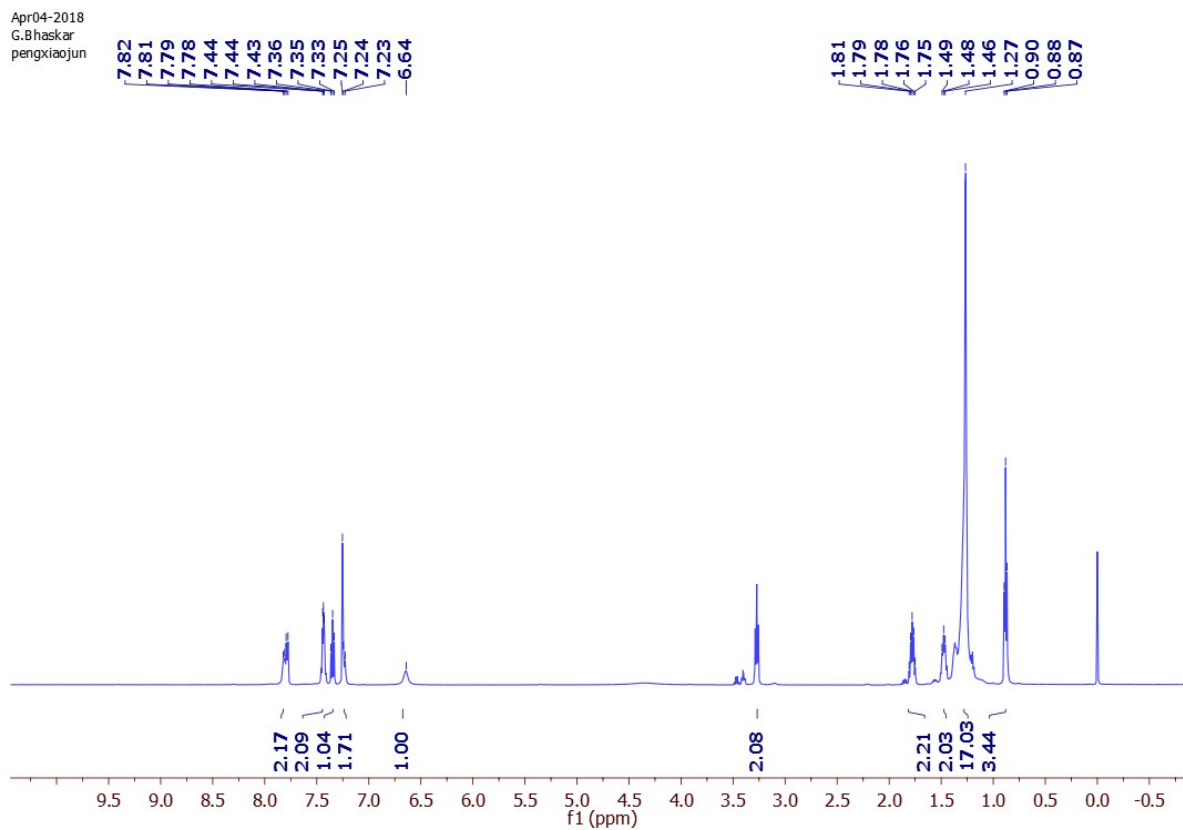


Figure S13. ^1H -NMR of **1** $\mathbf{R}_1 = \mathbf{NB-C12}$

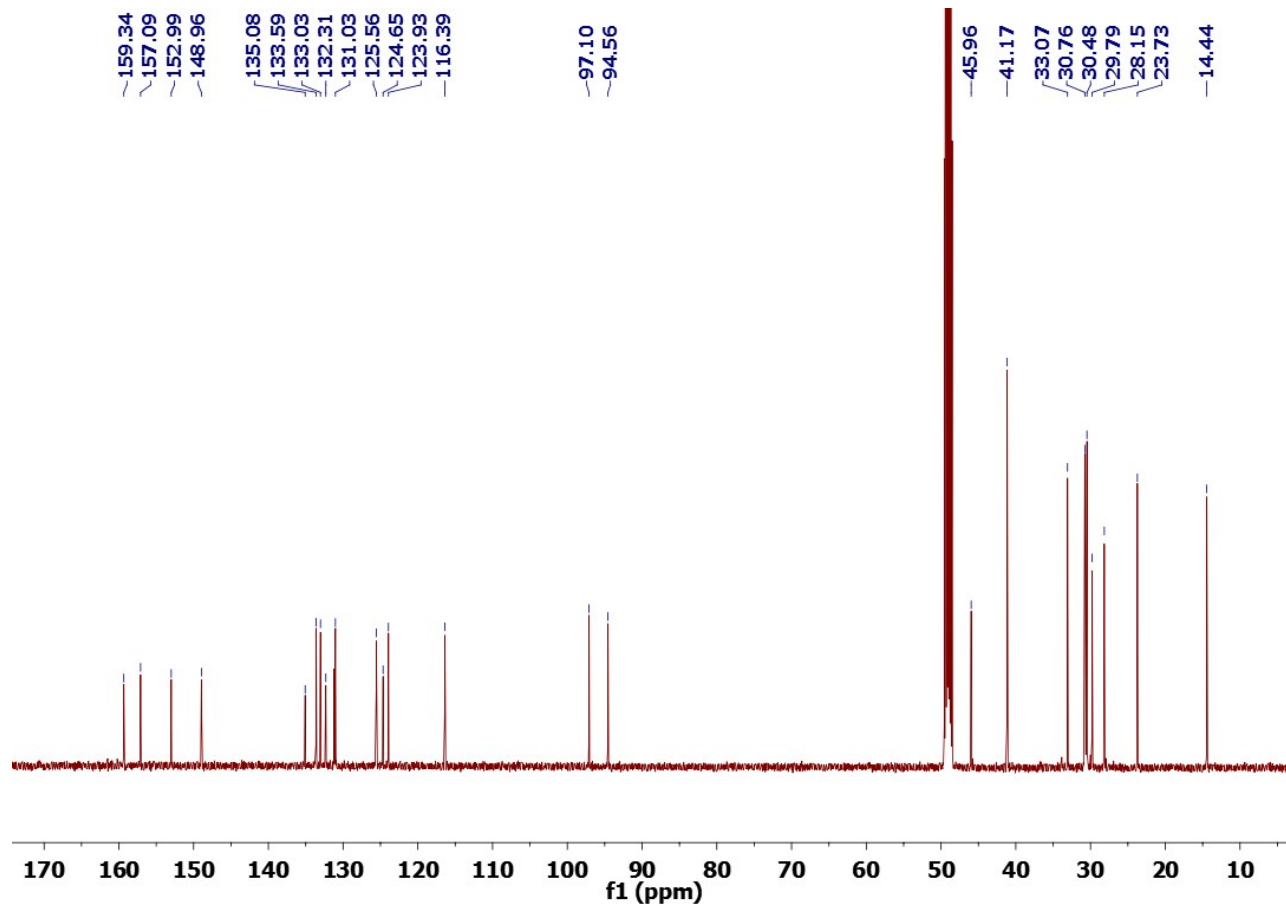


Figure S14. ^{13}C -NMR of **1** $\text{R}_1 = \text{NB-C12}$

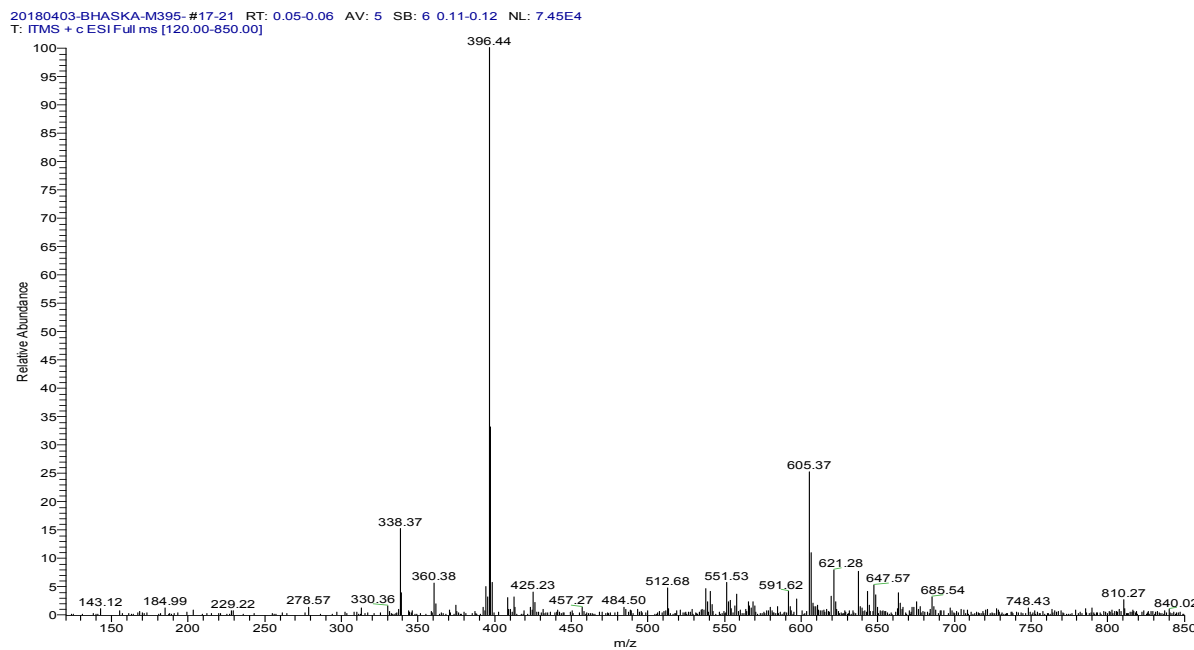


Figure S15. Mass of **2** $\text{R}_1 = \text{NB-C18}$

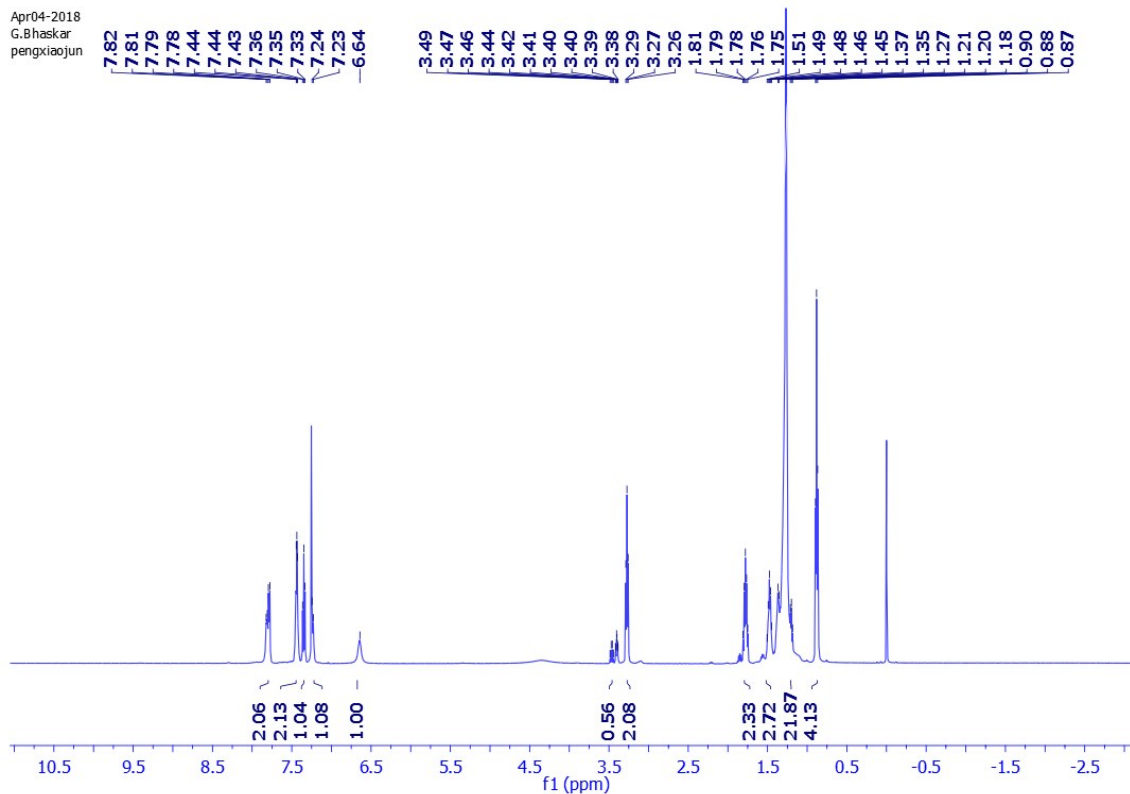


Figure S16. ^1H -NMR of **1** $\text{R}_1 = \text{NB-C18}$

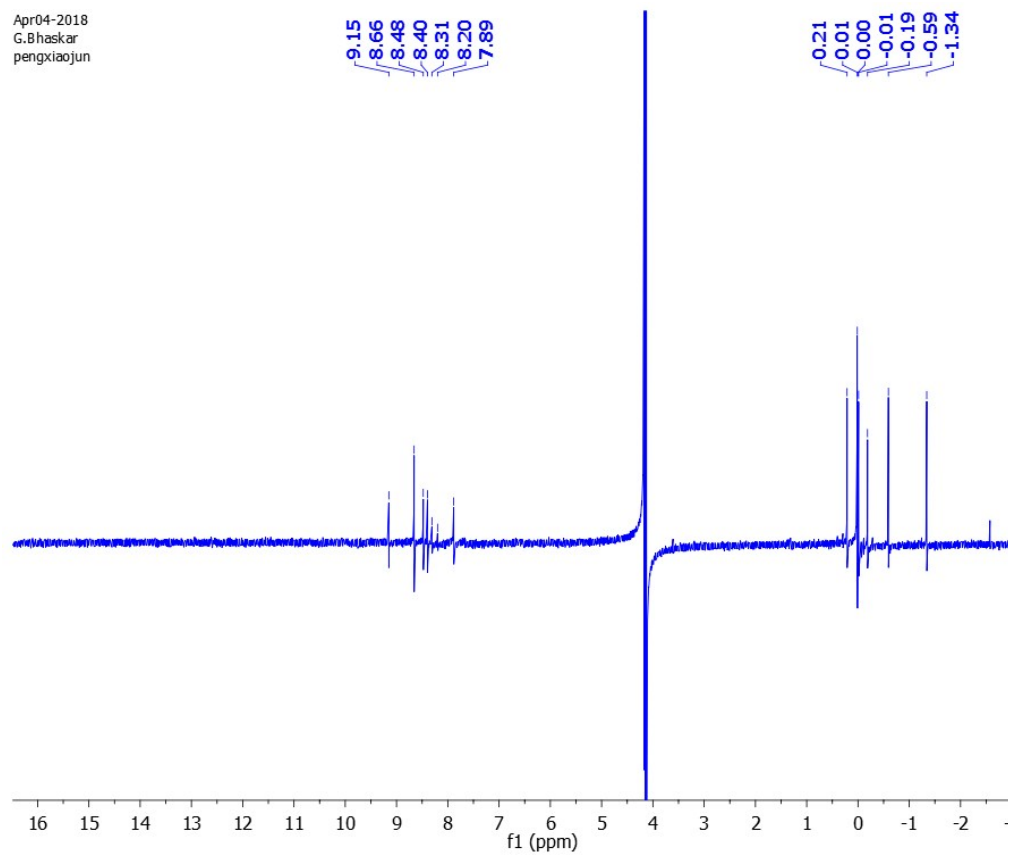


Figure S 17. ^{13}C -NMR of **1** $\text{R}_1 = \text{NB-C18}$

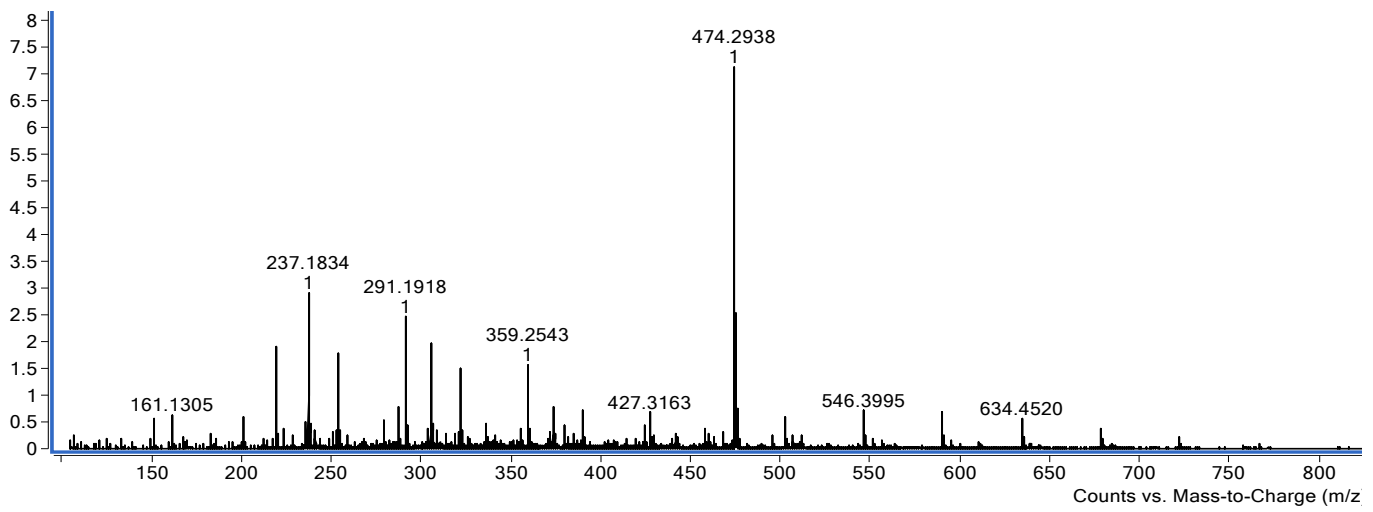


Figure S18. Mass of compound 2-R₂(Mt-NB-C12)

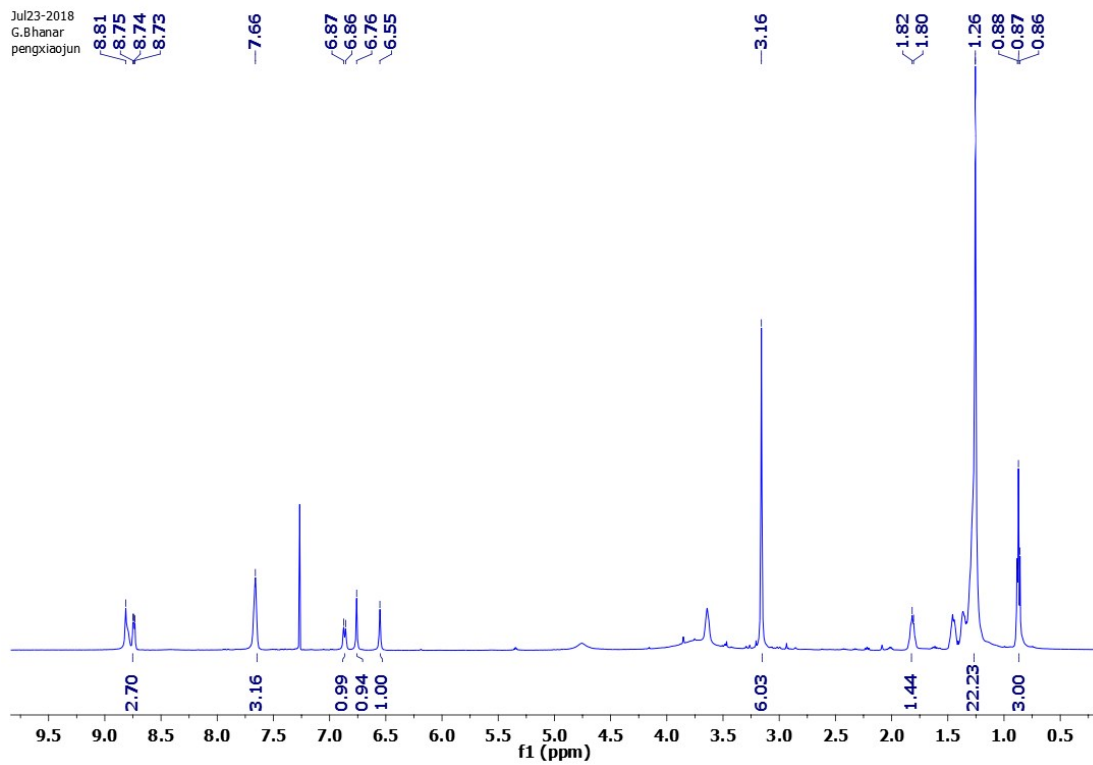


Figure S19. ¹H -NMR of compound 2-R₂(Mt-NB-C12)

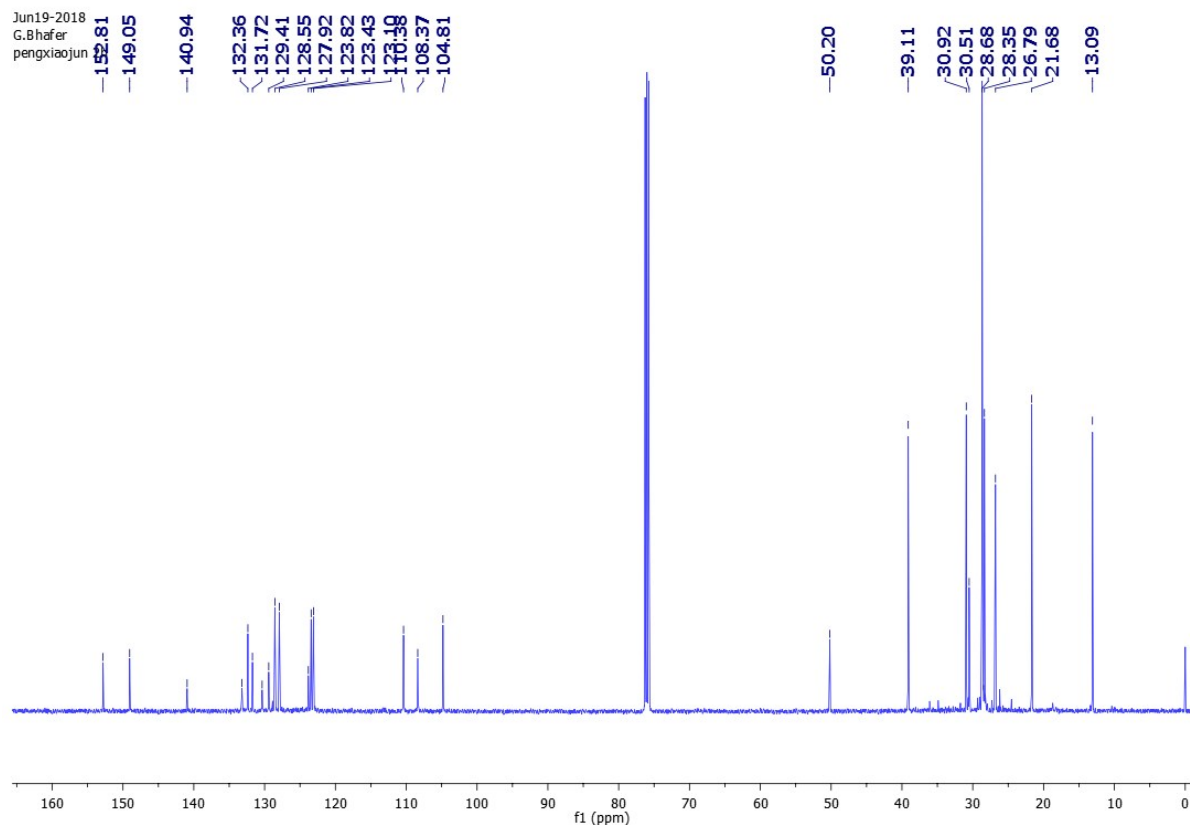


Figure S20. ^{13}C -NMR of compound 2-R₂(Mt-NB-C12)

20180710_Bhaskar_TSQ_MS_S2_180710140713 #10-38 RT: 0.10-0.35 AV: 14 SB: 20 0.00-0.12, 0.57-0.82 NL: 1.61E7
F: + c ESI Q1MS [100.000-1000.000]

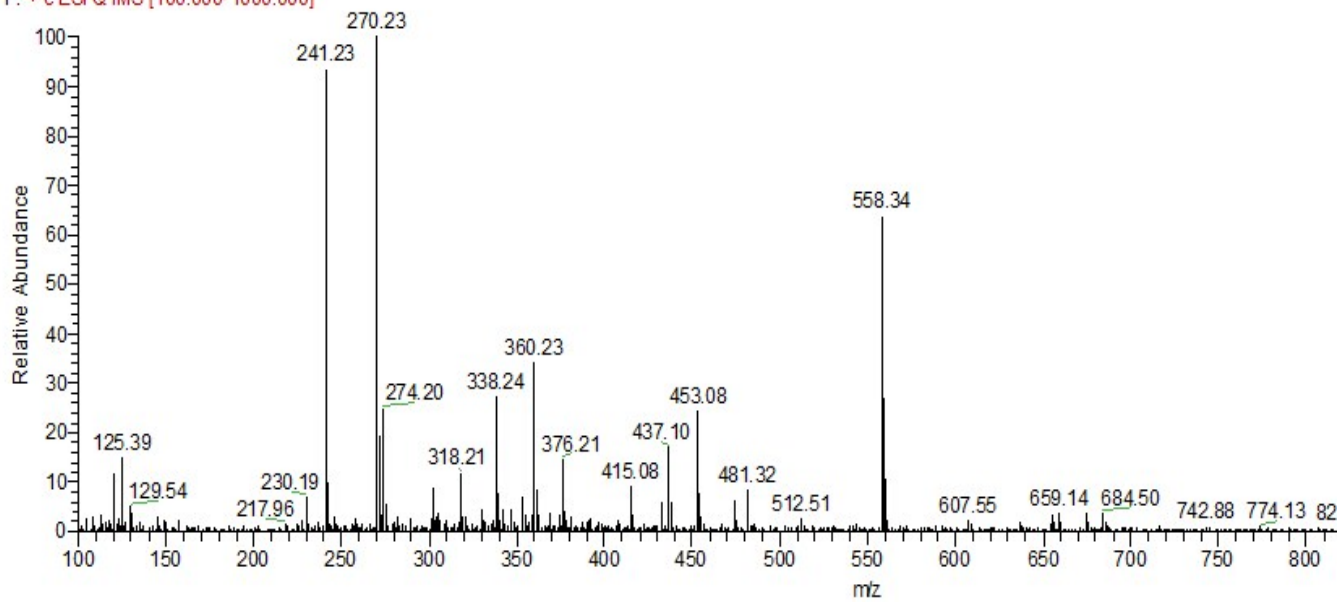


Figure S21. Mass of compound 3-R2 (Mt-NB-C18)

Jul11-2018
G.Bhaskar
peng xiao jun

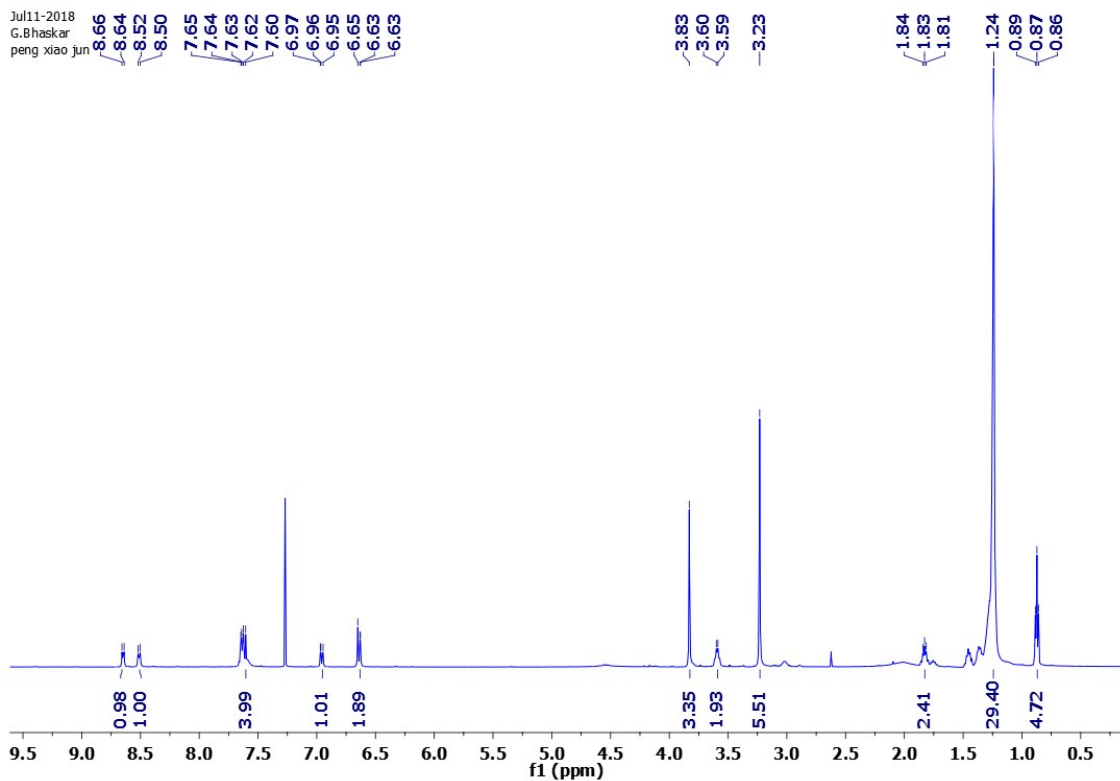


Figure S22. ¹H -NMR of compound 3-R₂(Mt-NB-C18).

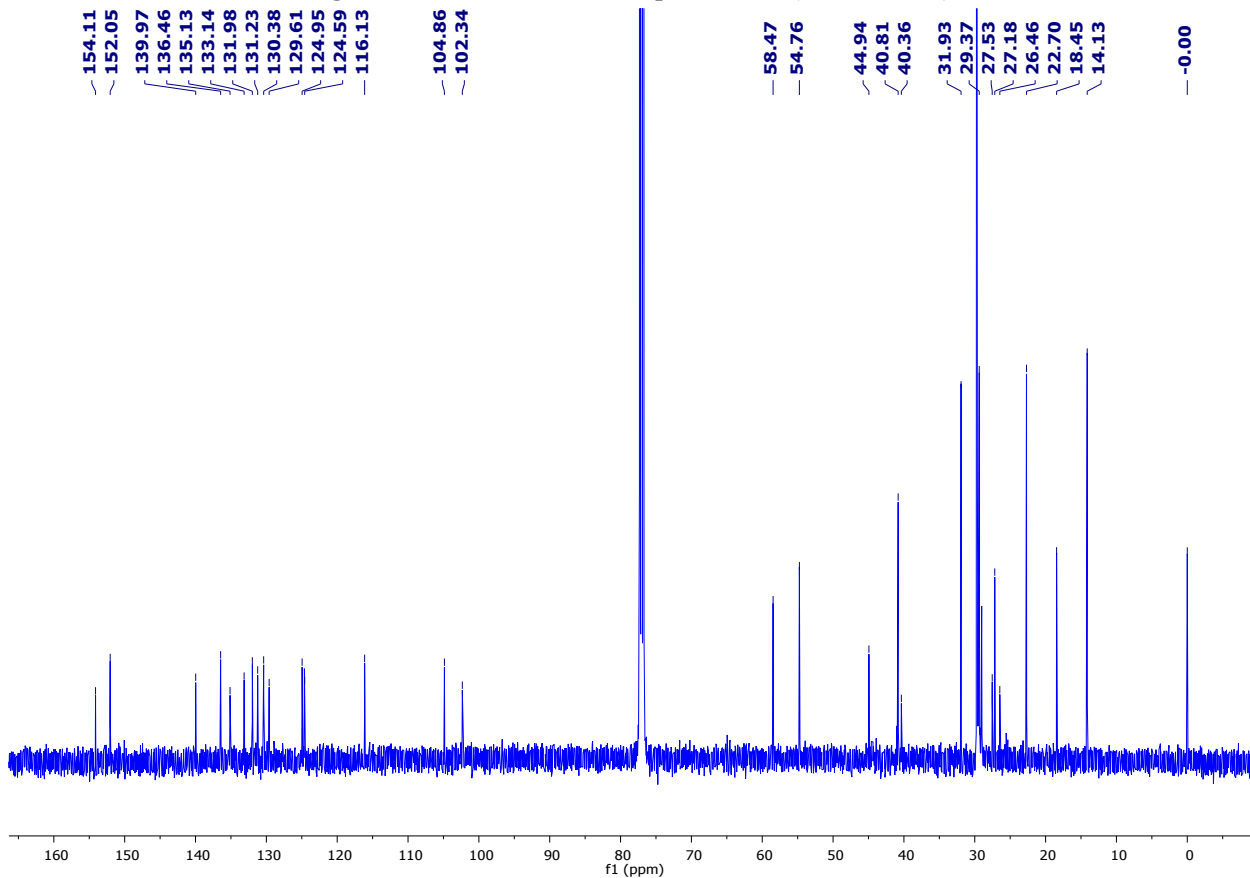


Figure S23. ¹³C -NMR of compound 3-R₂(Mt-NB-C18)

20180529-BHASKA-2 #30-31 RT: 0.83-0.86 AV: 2 SB: 5 0.94-1.00 , 0.01-0.01 NL: 1.02E7
T: FTMS + p ESI Full ms [120.00-1100.00]

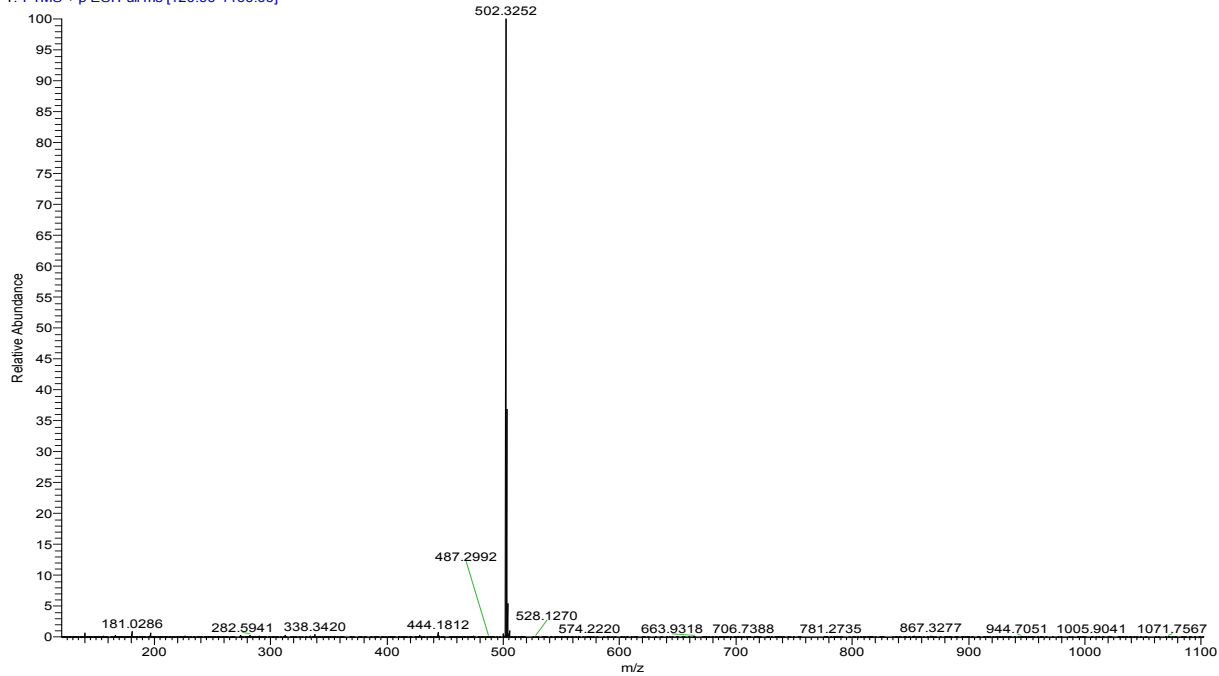


Figure S24. Mass of compound 4-R₁ (Et-NB-C12)

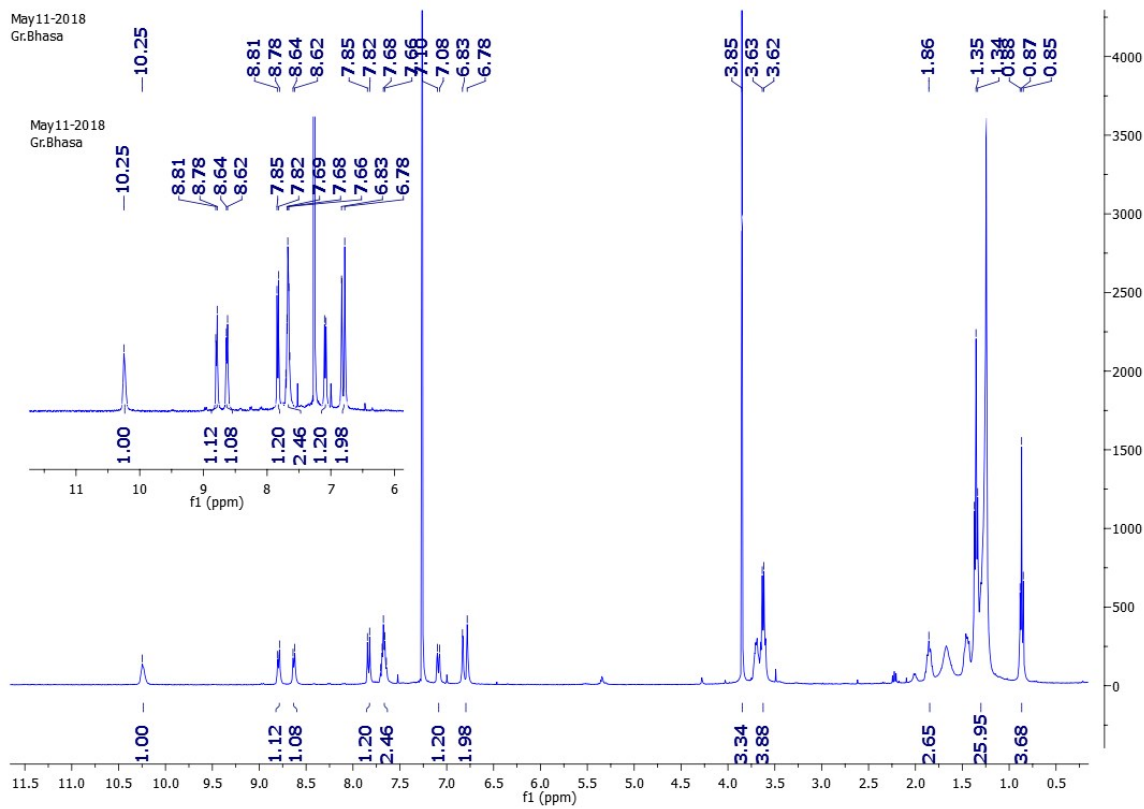


Figure S25. ^1H -NMR of compound 4-R1(Et-NB-C12)

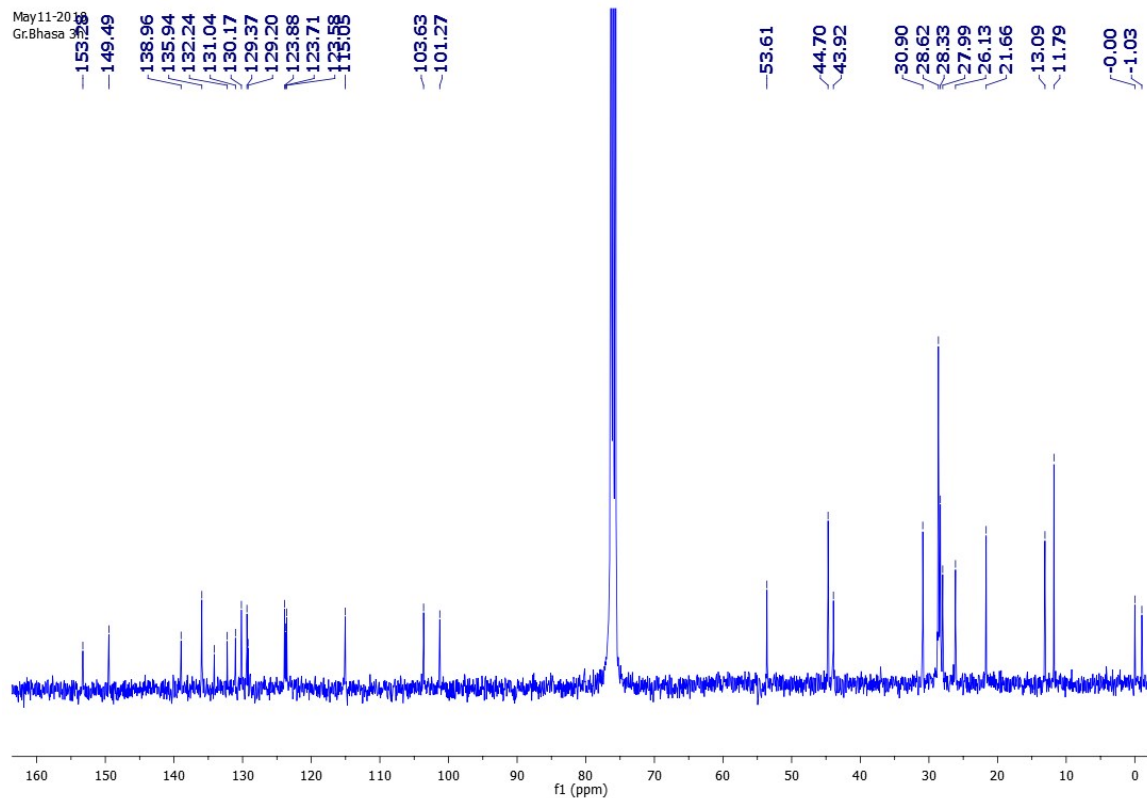


Figure S26. ^{13}C -NMR of compound 4-R₁(Et-NB-C12)

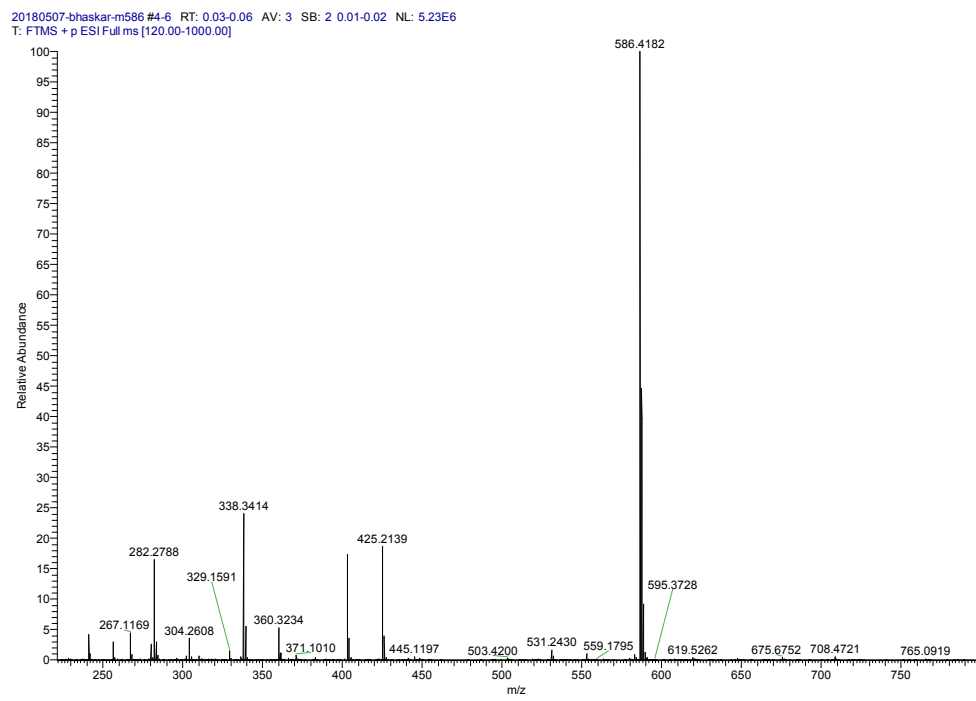


Figure S27. Mass of compound 5-R1 (Et-NB-C18)

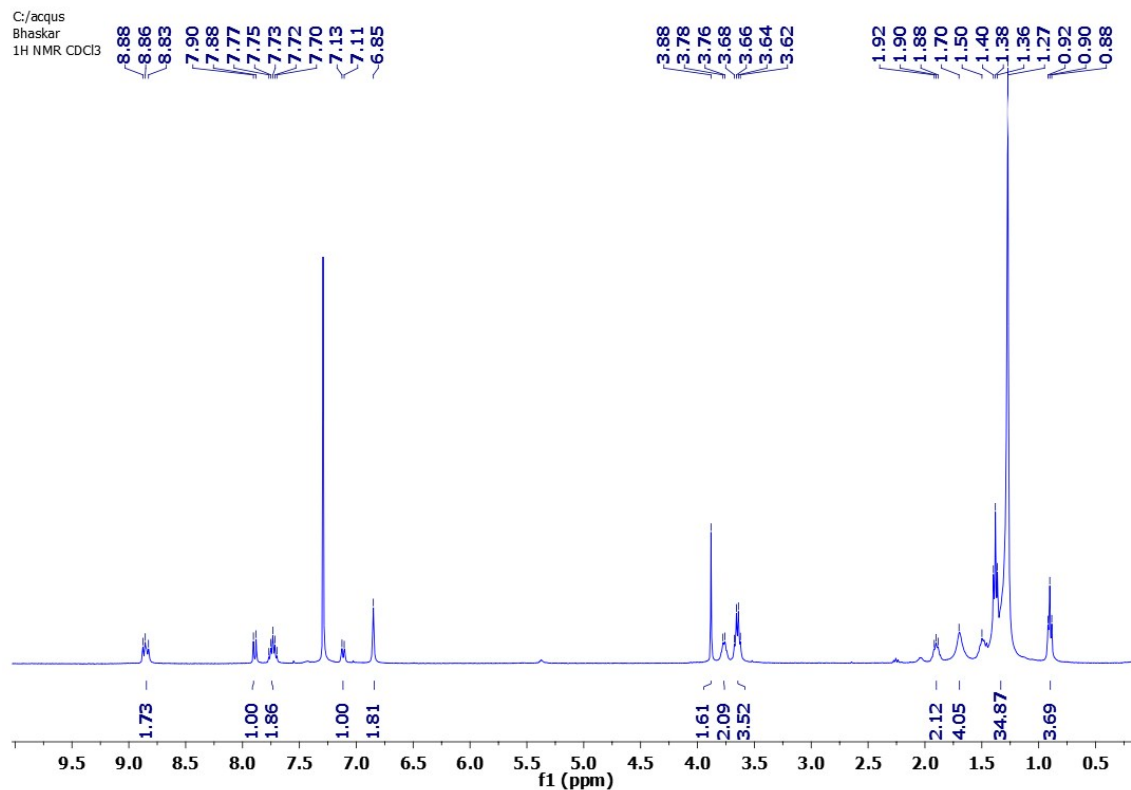


Figure S28. ¹H -NMR of compound 5-R₁(Et-NB-C18)

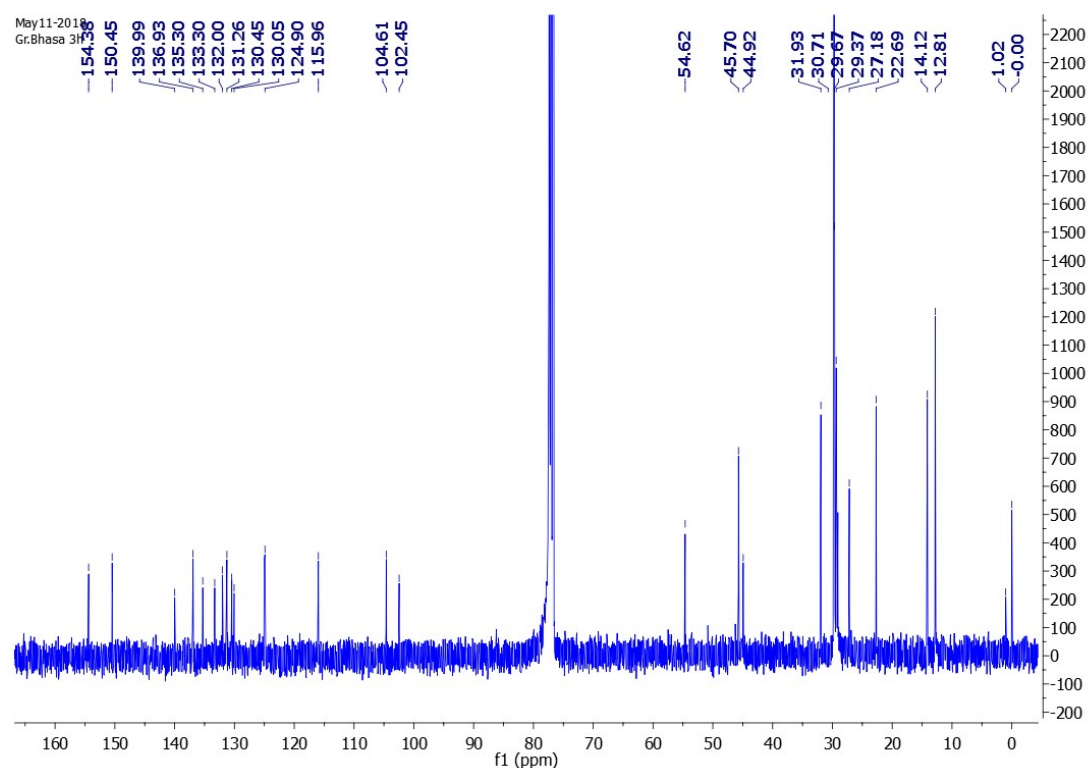


Figure S29. ¹³C-NMR of compound 5-R₁(Et-NB-C18)

BHASKAR-M460-01 #40-51 RT: 0.11-0.14 AV: 12 SB: 10 0.83-0.86 NL: 1.92E6
T: ITMS + c ESI Full ms [200.00-1000.00]

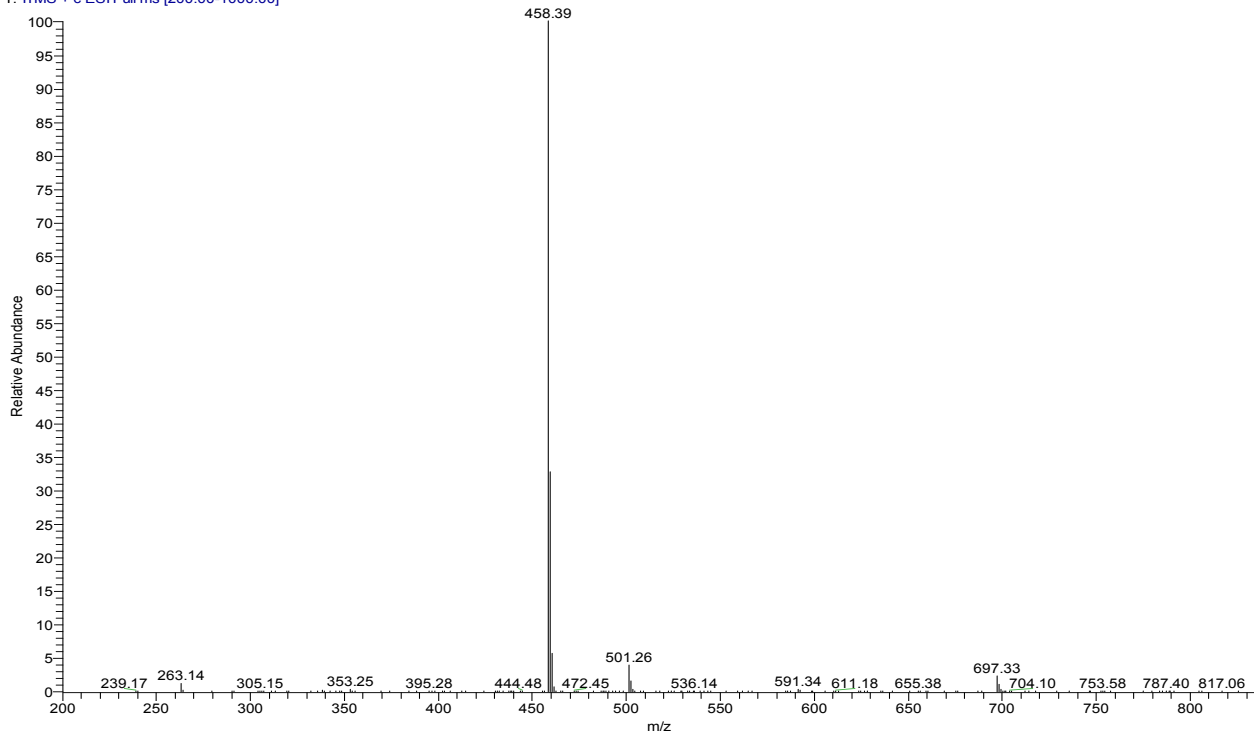


Figure S30. Mass of compound 6-R1(Mt-NB-O-C12)

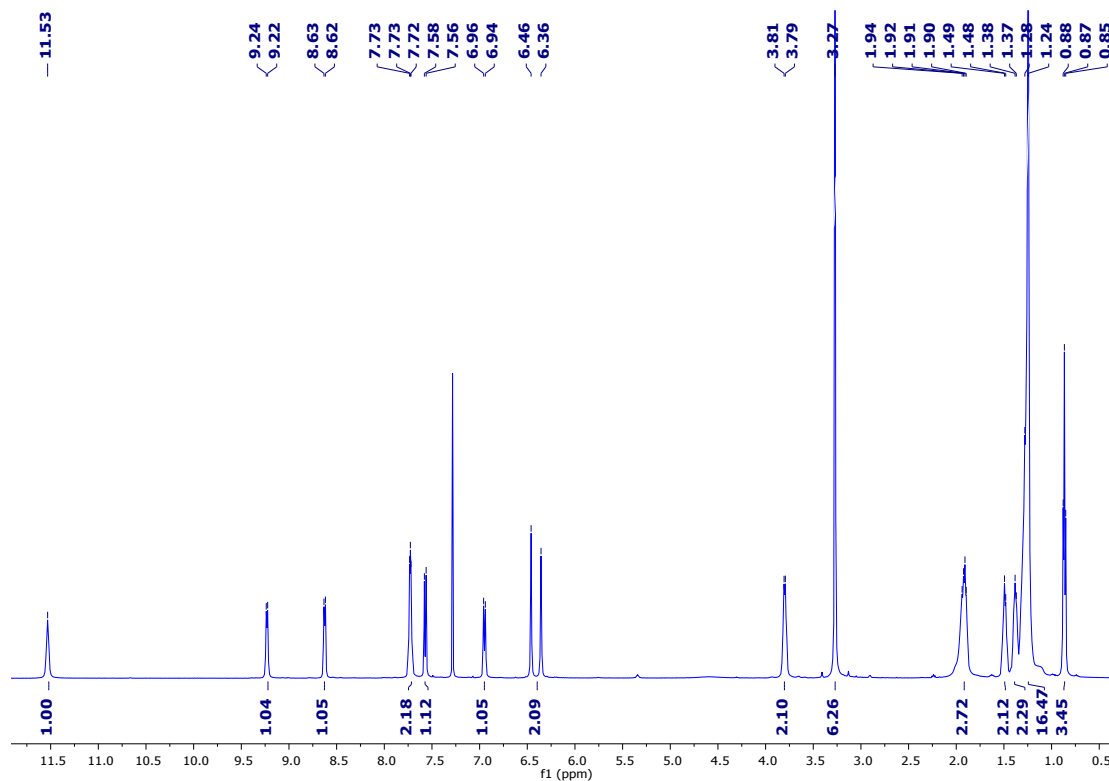


Figure S31. ^1H -NMR of compound 6-R1(Mt-NB-O-C12)

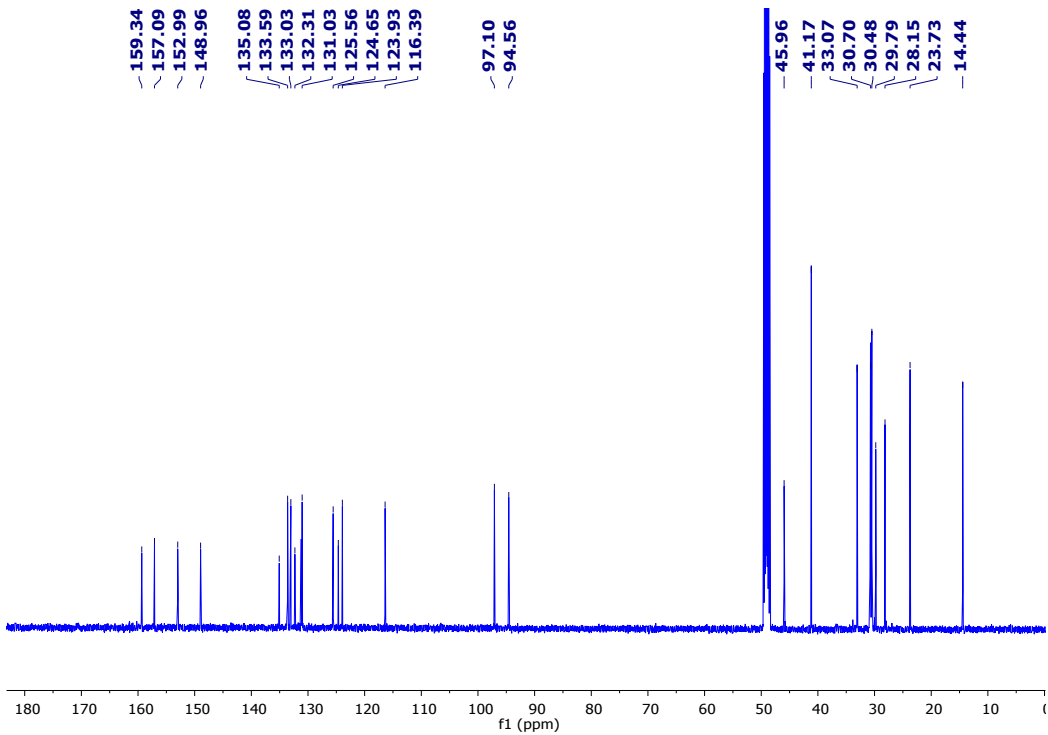


Figure S32. ¹³C-NMR of compound 6-R₁(Mt-NB-O-C12)